Murine double minute 2 as a therapeutic target for radiation sensitization of lung cancer

Carolyn Cao,[1] Eric T. Shinohara,[1] Kenneth J. Niermann,[2] Edwin F. Donnelly,[2] Xinping Chen,[1] Dennis E. Hallahan,[1] and Bo Lu[1]

Departments of [1]Radiation Oncology, and [2]Radiology, Vanderbilt Ingram Cancer Center, Vanderbilt University School of Medicine, Nashville, Tennessee

Abstract

Murine double minute 2 (MDM2) inhibits p53-mediated functions, which are essential for therapies using DNA-damaging agents. The purpose of this study was to determine whether MDM2 inhibition enhances the radiosensitivity of a lung cancer model. The effects of MDM2 inhibition on tumor vasculature were also studied. Transient transfection of H460 lung cancer cells and human umbilical vascular endothelial cells (HUVEC) with antisense oligonucleotides (ASODN) against MDM2 resulted in a reduced level of MDM2 and increased levels of p21 and p53. Clonogenic assays showed that inhibition of MDM2 greatly decreased cell survival following irradiation. Quantification of apoptotic cells by 7-aminoactinomycin D staining and of senescent cells by X-gal staining showed that both processes were significantly increased in H460 cells treated with MDM2-specific ASODN and radiation. H460 xenografts that were treated with MDM2 ASODN plus radiotherapy also showed significant growth delay ($P < 0.001$) and increased apoptosis by terminal deoxynucleotidyl transferase–mediated nick end labeling staining. HUVECs transfected with MDM2-specific ASODN showed impaired viability and migration with decreased tube formation. Doppler studies showed that tumor blood flow was compromised when H460 xenografts were treated with MDM2-specific ASODN and radiation. A combination of radiotherapy and inhibition of MDM2 through the antisense approach results in improved tumor control in the H460 lung cancer model. This implies that a similar strategy should be investigated among patients with locally advanced lung cancer, receiving thoracic radiotherapy. [Mol Cancer Ther 2005;4(8):1137–45]

Introduction

The murine double minute 2 (MDM2) oncogene is overexpressed in a number of human cancer cell lines and is associated with a poor clinical prognosis (1). Studies indicate that MDM2 has a critical role in regulating p53 response to DNA-damaging therapies (2, 3). Therefore, p53-targeted therapy can be affected by altering MDM2 function (4). MDM2 contains a p53-binding domain for ubiquitination and is known to regulate p53 expression (4–7). Recently, attenuation of MDM2 function has been associated with increased response to DNA damage in prostate (8), thyroid medullary carcinoma (9), and breast cancer (1).

However, MDM2 has also been shown to have effects on cell cycle arrest and apoptosis independent of p53. p53-independent activation of p21 by MDM2 has been shown (5, 10). p21 is associated with modulation of cell proliferation, differentiation, senescence, and apoptosis (11). Studies showed that MDM2 may inhibit p21, and by inhibiting MDM2, the antiproliferative and apoptotic effects of p21 may be potentiated (5).

Antisense oligonucleotides (ASODN) specifically block protein formation by inhibiting mRNA translation. ASODN are appealing because they can be rationally designed, are relatively inexpensive, and can be very specific. There are several ways in which ASODN can be used to block translation. For instance, a short sequence of bases (as short as 13–25 bases is specific; refs. 12, 13) can be used to specifically hybridize to mRNA in areas for ribosomal binding (12–14), which are usually the 5′ untranslated region or the AUG start codon (14). This prevents ribosomal binding and translation of the mRNA. An ASODN can also hybridize to mRNA forming a double-stranded duplex that is then cleaved by RNase-H. The advantage of this technique is that after cleavage, the ASODN is free to associate with another strand of mRNA allowing one ASODN to degrade several mRNA strands. Any sequence within the mRNA can be used as a target for the ASODN, giving it a variety of areas to target (14). ASODN can also be used to target the capping and polyadenylations sites of mRNA, which destabilizes it. ASODN can also target splicing regions to prevent maturation of the mRNA (15). Advantages of ASODN are that they target a specific protein, prevent formation of protein, and have a low toxicity.

Oligonucleotides against MDM2 have been used to inhibit MDM2 (1, 4, 8, 16) and to increase expression of p53 and p21 in numerous cancer cell lines (4). Inhibition of MDM2 has been shown to sensitize breast cancer to

Received 12/7/04; revised 5/16/05; accepted 6/14/05.

Grant support: Vanderbilt Discovery grant; Vanderbilt Physician Scientist grant; Mesothelioma Applied Research Foundation grant; and DOD grants PC031161, DOD BC030542, R01-CA88076, R01-CA89674, and T-32 CA93240.

The costs of publication of this article were defrayed in part by the payment of page charges. This article must therefore be hereby marked advertisement in accordance with 18 U.S.C. Section 1734 solely to indicate this fact.

Note: C. Cao and E.T. Shinohara contributed equally to this work.

Requests for reprints: Bo Lu, Department of Radiation Oncology, Vanderbilt University, 1301 22nd Avenue South, B-902 The Vanderbilt Clinic, Nashville, Tennessee 37232-5671. Phone: 615-343-9233; Fax: 615-343-3075. E-mail: bo.lu@vanderbilt.edu

doi:10.1158/1535-7163.MCT-04-0327

chemotherapeutics and sensitizes thyroid carcinoma to ionizing radiation (1, 9). However, it is not known which type of cell death mediates the MDM2-targeted radiosensitization and it is not clear whether MDM-2 ASODN also enhances the antivascular effects of radiotherapy. In this study, MDM2-specific ASODN was used to determine whether and how it sensitizes lung cancer to γ irradiation. Our results suggest that MDM2 inhibition sensitized the H460 lung cancer model to irradiation via induction of apoptosis and senescence as well as by enhancing the antivascular effects of radiation.

Materials and Methods

Cell Culture

Human umbilical vascular endothelial cells (HUVEC) were obtained from Clonetics (San Diego, CA) and maintained in EBM-2 medium supplemented with EGM-2 MV single aliquots (BioWhittaker, Walkersville, MD). H460 lung carcinoma cells were obtained from the American Type Culture Collection (Rockville, MD) and maintained in RPMI 1640 with 10% FCS and 1% penicillin/streptomycin. Irradiation (0–6 Gy) was given via ^{137}Cs irradiator (J.L. Shepherd and Associates, Glendale, CA).

ASODN Transfection

ASODNs were synthesized as described previously (TriLink BioTechnologies, San Diego, CA, ref. 10) using the following sequences: 5′-UGACACCTGTTCTCACUCAC-3′ and a mismatch control was synthesized using 5′-UGTCACCCTTTTTCATUCAC-3′. Underlined nucleotides are 2′-*O*-methoxyethyl modified. All internucleotide linkages are phosphorothioate. Subconfluent H460 or HUVEC cells were transfected with Lipofectin (Life Technologies, Gaithersburg, MD) and oligonucleotides in Opti-MEM medium (Life Technologies) at a ratio of 3 μL Lipofectin per milliliter of medium per 100 nmol/L oligonucleotide. After 4 hours of incubation, the medium was changed.

Western Immunoblots

Cells were transfected with anti-MDM2 oligonucleotide or missense oligonucleotide overnight. Cells were irradiated with 5 Gy and incubated for 0 and 24 hours at 37°C. Ice-cold PBS was used to wash cells twice before addition of lysis buffer. Protein concentrations were quantified by the Bio-Rad method. Equal amounts of protein were loaded into each well and separated by 10% or 15% SDS-PAGE and transferred onto nitrocellulose membranes. Blots were incubated with primary antibodies [MDM2, p53, p21 (Santa Cruz Biotechnologies, Santa Cruz, CA); and β-actin (Sigma, St. Louis, MO), 1:1,000] overnight at 4°C. Goat anti-rabbit or goat anti-mouse IgG (1:1,000; Santa Cruz Biotechnologies) secondary antibody was incubated for 1 hour at room temperature. Immunoblots were developed using the enhanced chemiluminescence detection system (Amersham, Piscataway, NJ) according to the manufacturer-specified protocol and autoradiography.

Measurement of Apoptosis

Percent apoptosis was measured by using 7-aminoactinomycin D (Molecular Probes, Eugene, OR) with flow cytometry. Cells were plated into 25 cm^2 flasks (4×10^5) for each treatment group. After 24 hours of incubation at 37°C, cells were transfected with anti-MDM2 or missense oligonucleotides for 5 hours. Cells in irradiation groups were irradiated with 2 Gy and incubated at 37°C. Twenty-four hours after irradiation, cells were trypsinized (keeping all floating cells). Cells were resuspended in PBS plus 1% paraformaldehyde and analyzed using FACScan. Cells with intermediate levels of 7-aminoactinomycin D staining were scored as apoptotic.

Measurement of Senescent Cells

H460 cells were transfected with either anti-MDM2 or missense oligonucleotides and incubated at 37°C overnight. Transfected cells were treated with 0.5 Gy. Three days after irradiation, cells were stained with X-gal. The percentage of senescent cells was determined from each set of 200 cells counted. This was done in triplicate and then these percentages were averaged to determine an overall average of senescent cells.

In vitro Clonogenic Assay

H460 human lung carcinoma cells were trypsinized and counted. Cells were serially diluted to appropriate concentrations and plated into 25 cm^2 flasks in 5 mL medium in triplicate. Anti-MDM2 and missense oligonucleotide stock solutions were made in sterile water at 1 mmol/L. Oligonucleotide concentrations were 300 nmol/L in all of the experiments.

Oligonucleotide transfections of anti-MDM2 and missense oligonucleotides were done 24 hours after plating. Cells in radiation groups were irradiated using a ^{137}Cs irradiator. Dose rate was 1.8 Gy/min and doses of 0, 2, 4, and 6 Gy were given. After treatment, cells were incubated at 37°C for 8 days. Cells were then fixed for 15 minutes with methanol/acetic acid (3:1) and stained for 15 minutes with 0.5% crystal violet (Sigma) in methanol. Colonies were counted with a cutoff of 50 viable cells to be scorable. Radiation dose enhancement ratio was calculated as the dose (in Gy) for radiation alone divided by the dose for radiation plus drugs (normalized for drug toxicity) to obtain a surviving fraction of 0.25.

Tumor Volume Assessment

H460 cells were used as a xenograft model in female athymic nude mice (nu/nu, 5 to 6 weeks old; Harlan Sprague-Dawley, Inc., Indianapolis, IN). Institutional Animal Care and Use Committee approval for an animal protocol for animal care and use was obtained before nude mouse experiments. A suspension of 2×10^6 cells in 50 μL volume was injected s.c. into the left posterior flank of nude mice. Tumors were grown for 8 days until average tumor volume reached 0.2 cm^3. Mice were then stratified into groups (five mice per group) so that the mean tumor volume in each group was comparable. Treatment groups consisted of untreated control (sterile water), missense oligonucleotide treatment alone, missense oligonucleotide transfected before radiation treatment, anti-MDM2 oligonucleotide treatment alone, and anti-MDM2 oligonucleotide transfected before radiation treatment. Oligonucleotide was given on treatment days 1 to 6 via i.p. injection, 1 hour

before irradiation, at a dose of 10 mg/kg. The radiation groups received 10 Gy of radiation fractionated over 5 consecutive days (from days 2 to 6) using an X-ray irradiator (300 kV, 10 mA at a rate of 205 cGy/min). The field was adjusted to cover the entire tumor with an adequate (~1 cm) border and the X-ray source was positioned 50 cm from the tumor. The remainder of the body was shielded with lead blocks.

Tumors were measured twice or thrice weekly in three perpendicular dimensions using a vernier caliper (17, 18). Measurements began on treatment day 1 and every 2 days until the tumor volumes became 10% of the body size, ~2.5 to 4 weeks depending on treatment group. Tumor volumes were calculated using a formula that was derived from the formula for an ellipsoid, $a \times b \times c / 2$. Data was calculated as the percentage of the original (day 1) tumor volume and graphed as tumor volume change ± SD for each treatment group. Growth delay (GD) was calculated as the time for treated tumor to reach 2.0 cm^3 minus the time for control tumors to reach 2.0 cm. The enhancement factor (EF) was then determined as follows:

$$EF = \frac{GD_{Drug+XRT} - GD_{Drug}}{GD_{XRT}}$$

where ''Drug'' represents anti-MDM2 treatment and ''XRT'' represents missense plus radiation treatment.

Endothelial Cell Morphogenesis Assay: Tube Formation

HUVECs were transfected with anti-MDM2 or missense oligonucleotides for 5 hours. The medium was changed after 1 hour and cells were treated with 3 Gy of γ irradiation. Cells were trypsinized and counted. They were seeded at 48,000 cells/well on 24-well plates coated with 300 μL of Matrigel (BD Biosciences, San Jose, CA). These cells undergo differentiation into capillary-like tube structures and were periodically observed using a microscope. After 24 hours, cells were stained with H&E and photographs were taken via a microscope. The average number of tubes for three separate microscopic fields (×100) and representative photographs were taken.

3-(4,5-Dimethylthiazol-2-yl)-2,5-Diphenyltetrazolium Bromide Assay: Cell Viability

Briefly, cells were seeded at a density of 2,000 to 5,000 cells/well in 96-well plates grown overnight. They were subjected to various treatments. Forty-eight hours later, 3-(4,5-dimethylthiazol-2-yl)-2,5-diphenyltetrazolium bromide (MTT) was added (50 μg/well) for 4 hours. Solubilization of the converted purple formazan dye was accomplished by placing cells in 100 μL of 0.01 N HCl/10% SDS and incubating overnight at 37°C. The reaction product was quantified by absorbance at 570 nm. All samples were done in triplicate and data were analyzed by Student's t test.

Terminal Deoxynucleotidyl Transferase–Mediated Nick End Labeling Staining: Marker for Apoptosis

Terminal deoxynucleotidyl transferase–mediated nick end labeling (TUNEL) was done in the same four treatment groups as described above. Tumors were prepared as described above. Mice were sacrificed on day 6 of each treatment and tumors were collected and preserved in 10% paraformaldehyde. Tumors were then sent to a Vanderbilt Core facility for TUNEL staining. Photos were then taken using a microscope for apoptosis in xenografts treated with anti-MDM2 oligonucleotide, missense oligonucleotide, anti-MDM2 oligonucleotide and radiation, and missense oligonucleotide and radiation. The number of apoptotic cells was counted in three separate microscopic fields (×100) for each group. This was done in triplicate and the three counts were then averaged for each group and graphed.

Doppler Imaging of Tumors

Blood flow within these tumors was quantified by power Doppler images after the third fraction of irradiation. Tumor blood flow was imaged with a 10 to 5 MHz linear Entos probe attached to a HDI 5000 (probe and HDI 5000 from ATL/Philips, Bothell, WA) as we have previously described (15). Power Doppler sonography images were obtained with the power gain set to 82%. A 20-frame cineloop sweep of the entire tumor was obtained with the probe perpendicular to the long axis of the lower extremity along the entire length of the tumor. Color area was quantified using HDI lab software (ATL/Philips). This software allows direct evaluation of power Doppler images cineloop raw. The color area was recorded for the entire tumor. Five mice were entered into each treatment group. Values for color area were averaged for each tumor set and treated groups were compared with controls with the unpaired Student's t test.

Statistical Analysis

We used the general linear model (logistic regression analysis) to test for associations between the numbers of apoptotic cells present in culture, clonogenic survival, tumor blood flow, and tumor volumes. We applied the Bonferroni method to adjust the overall significant level to 5% for the multiple comparisons in this study. All statistical tests were two-sided, and differences were considered statistically significant for $P < 0.05$. SAS software version 8.1 (SAS Institute, Inc., Cary, NC) was used for all statistical analyses.

Results

Treatment with MDM2 ASODNs and Radiation Up-Regulates p53 and p21 in H460 Cells but not in HUVECs

To determine how the molecular changes following radiation are affected by reduced MDM2 expression as a result of MDM2-specific ASODN, H460 lung cancer and HUVEC cells were treated with missense ASODN, anti-MDM2 oligonucleotide, missense ASODN with radiation, or anti-MDM2 oligonucleotide. Protein levels of MDM2, p53, and p21 were determined by Western blotting. As shown in Fig. 1, H460 cells pretreated with missense ASODN followed by 5 Gy showed an increase in MDM2, p53, and p21 expression at 24 hours, compared with H460 treated with missense ASODN alone. The radiation-induced increase in MDM2 was attenuated in cells pretreated with anti-MDM2 oligonucleotide. However, both p53 and p21 expressions still increased following combination treatment with MDM2 ASODN and 5 Gy of

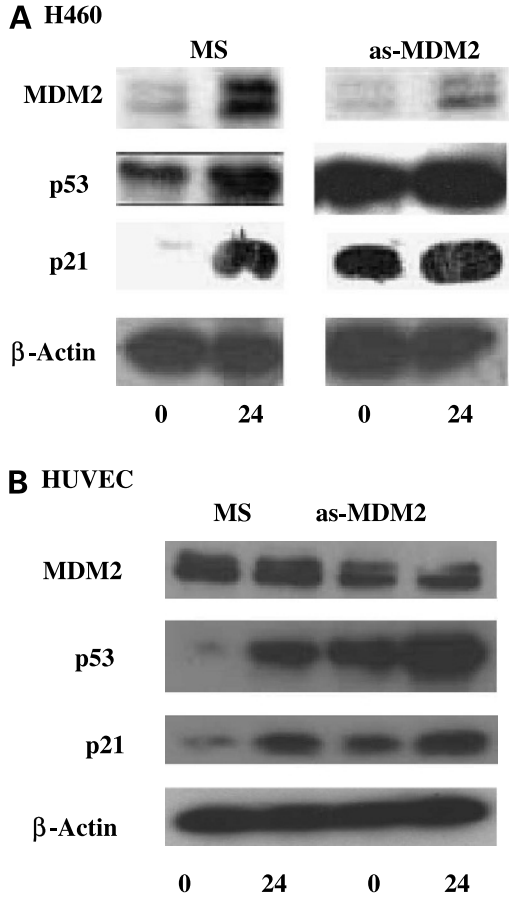

Figure 1. Inhibition of MDM2 results in increased p53 and p21 expressions in H460 lung cancer cells. Change in MDM2 levels in H460 and HUVEC cells in response to indicated doses of radiation was determined by Western blotting using anti-MDM2 antibody. **A,** H460 cells were transfected with anti-MDM2 (*as-MDM2*) or missense (*MS*) control oligonucleotide overnight. Cells were then irradiated with 5 Gy, collected at the indicated time points, and analyzed by Western blotting. MDM2, p53, and p21 were probed for. β-actin was probed to show equal loading of protein extracts. **B,** HUVECs were transfected with anti-MDM2 or missense oligonucleotide overnight and then irradiated with 5 Gy or untreated. MDM2 antibody was used to determine MDM2 expression and β-actin was used as a loading control.

radiation when compared with H460 treated with anti-MDM2 oligonucleotide alone. HUVEC pretreated with missense ASODN followed by radiation showed an increase in expression of p53 and p21, with MDM2 levels remaining relatively constant. HUVEC pretreated with anti-MDM2 oligonucleotide alone also had no appreciable difference in MDM2 expression compared with HUVEC treated with anti-MDM2 oligonucleotide followed by radiation. However, there was an appreciable increase in both p53 and p21 expressions in response to radiation and anti-MDM2 oligonucleotide treatment compared with those treated with anti-MDM2 oligonucleotide alone. In HUVEC pretreated with anti-MDM2, there was a decrease in MDM2 expression and a noticeable increase in p53 and p21 expressions compared with HUVEC treated with missense ASODN. β-actin was probed as a loading control.

Inhibition of MDM2 Sensitizes H460 Cells to Radiation by Increasing Apoptosis and Cell Senescence

To determine whether inhibition of MDM2 changes sensitivity of H460 lung cancer cells to radiotherapy, we examined cell death and survival of ASODN-treated cells following irradiation. The percentage of apoptotic cells was determined by flow cytometry analysis of 7-aminoactinomycin D–stained cells. As shown in Fig. 2A, missense oligonucleotide alone caused apoptosis in 5.6 ± 0.6% (mean ± SD) cells and radiation treatment increased this to 16 ± 1.3%. The anti-MDM2 oligonucleotide alone had a greater effect than the missense oligonucleotide with 18 ± 0.2% apoptotic cells. There was a significant increase in cells treated with anti-MDM2 oligonucleotide and irradiation with 29 ± 2% apoptotic cells compared with anti-MDM2 alone ($P < 0.05$).

Cell senescence following the various treatments described was determined by X-gal staining of β-galactosidase–expressing cells. Missense oligonucleotide caused 2.7 ± 0.2% and 7.0 ± 0.6% (mean ± SD) of senescent cells at 0 and 5 Gy, whereas anti-MDM2–treated cells showed significantly greater senescence with 5.3 ± 0.4% and 42.7 ± 1.5% ($P < 0.001$ missense compared with anti-MDM2 oligonucleotide) as shown in Fig. 2B.

Clonogenic assays were used to determine the impact of MDM2 inhibition on survival of H460 cells following irradiation. H460 cells were transfected with anti-MDM2 or missense oligonucleotide. Transfected cells and nontransfected controls were treated with 0, 2, 4, and 6 Gy irradiation. After 8 days, colonies were stained and counted to construct survival curves. As shown in Fig. 2C, H460 cells transfected with missense oligonucleotide showed some toxicity due to transfection. There was a decreased survival fraction across several points in H460 cells treated with MDM2 oligonucleotide and radiation. Dose enhancement ratio for anti-MDM2 oligonucleotide and radiation was 1.45. This suggests that MDM2 inhibition is able to radiosensitize H460 cells.

Inhibition of MDM2 Enhanced Radiation-Induced Tumor Regression in H460 Cells

To determine whether MDM2 inhibition enhances radiotherapy, a H460 xenograft model was established and tumor volumes were measured. Anti-MDM2 and missense oligonucleotides were given daily for 6 consecutive days to their respective treatment groups. Dose for both oligonucleotides was 10 mg/kg and given i.p. Starting on treatment day 2, 2 Gy was given to radiation groups 1 hour after oligonucleotide treatment for 5 consecutive days. A nontreated control was used to determine the nonspecific effects of oligonucleotides. Tumors were measured twice to thrice a week over 32 days. Growth delay was calculated as the time for treated tumor to reach 2.0 cm^3 minus the time for control tumors to reach 2.0 cm^3. As shown in Fig. 3, treatment with anti-MDM2 and missense oligonucleotides alone resulted in no significant difference between their tumor growth and the control mouse group. Radiation therapy caused a growth delay of

8 days. Administration of anti-MDM2 oligonucleotide followed by radiotherapy increased the delay up to 16 days. Enhancement factor for anti-MDM2 was 2.03 ($P \leq 0.001$). To determine the extent of apoptosis in these tumors, TUNEL staining was done on these tumor sections. Representative photos were taken via microscope and apoptotic cells were counted on three separate, randomly selected fields (×100) and averaged. Missense oligonucleotide alone averaged 1 ± 0.0 apoptotic bodies per field compared with 2.33 ± 0.9 in anti-MDM2 oligonucleotide-treated tumors. Missense oligonucleotide with radiation had 3.33 ± 0.3 and anti-MDM2 oligonucleotide with radiation had 7.33 ± 1.2 as shown in Fig. 4.

Inhibition of MDM2 Sensitizes Vascular Endothelium to Radiation Injury

Because the tumor vascular endothelium comes into contact with the ASODNs before they can reach the tumor cells, we determined the potential effects of various ASODNs on tumor vasculature. HUVECs were transfected with anti-MDM2 or missense oligonucleotides and irradiated with 0 (control) or 3 Gy (irradiated). Endothelial cell morphogenesis assay allows quantification of the ability of HUVECs to produce tubular structures *in vitro* as shown in Fig. 5. Tubules in three randomly selected fields (×100) were counted and averaged. HUVECs transfected with anti-MDM2 and irradiated with 3 Gy formed significantly reduced tubules [6 ± 1.8 microtubules (mean ± SD) per ×100 high power field]. Anti-MDM2 oligonucleotide alone exhibited some effect on microtubule formation with 20 ± 1.2 microtubules per high power field. In contrast, missense oligonucleotide plus irradiation formed 32 ± 1.5 microtubules, whereas missense oligonucleotide alone formed 57 ± 2.1 microtubules per high power field ($P < 0.001$). To determine whether the decrease in tubule formation resulted from a decrease in cell survival, HUVEC viability in response to treatment with anti-MDM2 and radiation was determined using the MTT assay. HUVEC were then transfected as described in the morphogenesis assay. As shown in Fig. 5C, HUVECs treated with both MDM2 ASODN and radiation had the least viable cells following the treatment.

Inhibition of MDM2 Causes Decreased Tumor Blood Flow in H460 Tumors Treated with Radiation

In vivo analysis of tumor blood flow was done using power Doppler images imaging on treatment days 1 and 5 on tumors described in Materials and Methods. Shown in Fig. 6 are representative examples of Doppler images from each experimental group of mice. Values from treatment day 1 (pretreatment) and day 6 (posttreatment) are graphed. Color Doppler sonography was used to determine the *in vivo* effects of these various treatment regimens on tumor neovascularization over the course of treatment. At the onset of treatment, all tumors in the respective groups

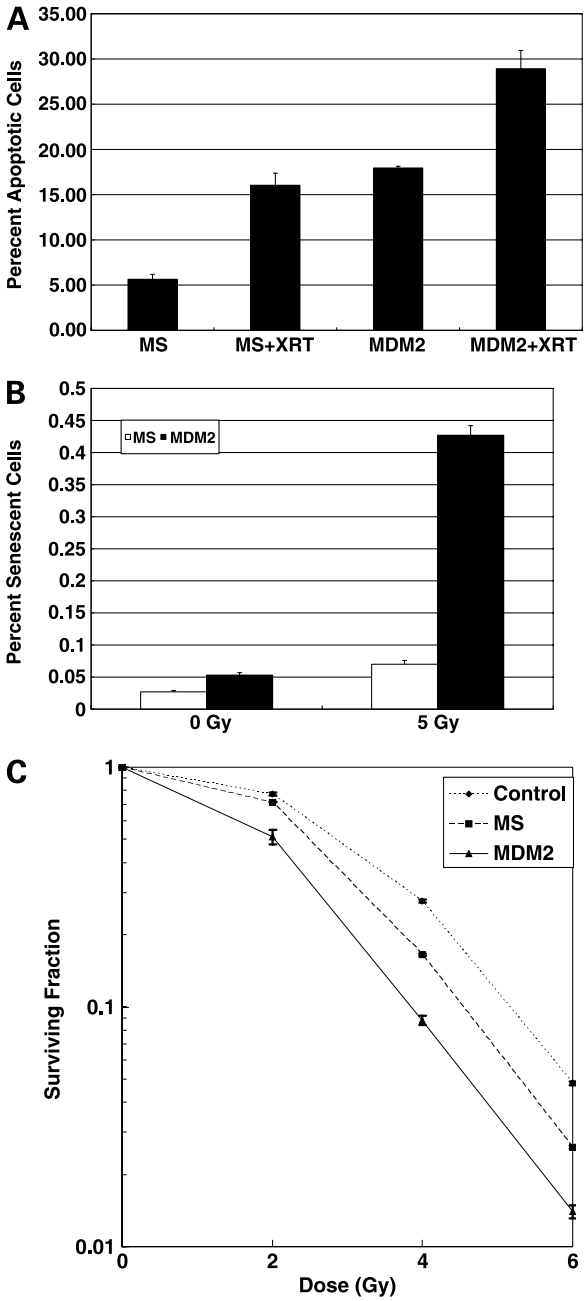

Figure 2. Inhibition of MDM2 sensitizes H460 cells to radiation by increasing apoptosis and senescence. **A,** H460 cells transfected with anti-MDM2 or missense oligonucleotide were treated with either 0 or 2 Gy irradiation 24 h later. Cells were stained with 7-aminoactinomycin D. Shown are the percentages of apoptotic cells in each treatment group determined by flow cytometry of 7-aminoactinomycin D–stained cells. *Columns,* mean from three repeated experiments; *bars,* SD. **B,** H460 cells transfected with either anti-MDM2 or missense oligonucleotide were treated with 0 or 5 Gy irradiation. Two hundred cells were counted in triplicate for each group and the number of X-gal cells per 200 was used to calculate the percentage of senescent cells. *Columns,* mean from three repeated experiments; *bars,* SD. **C,** H460 cells transfected with anti-MDM2 or missense oligonucleotide were treated with 0, 2, 4, and 6 Gy irradiation. The plating efficiency for untreated cells was 70%. *Points,* mean; *bars,* SD. SD values for 2 Gy were 0.0098, 0.0032, and 0.037 for control, missense, and MDM2, respectively. SD values for 4 Gy were 0.0041, 0.0015, and 0.0038 for control, missense, and MDM2, respectively. SD values for 6 Gy were 0.009, 0.0003, and 0.0009 for control, missense, and MDM2, respectively.

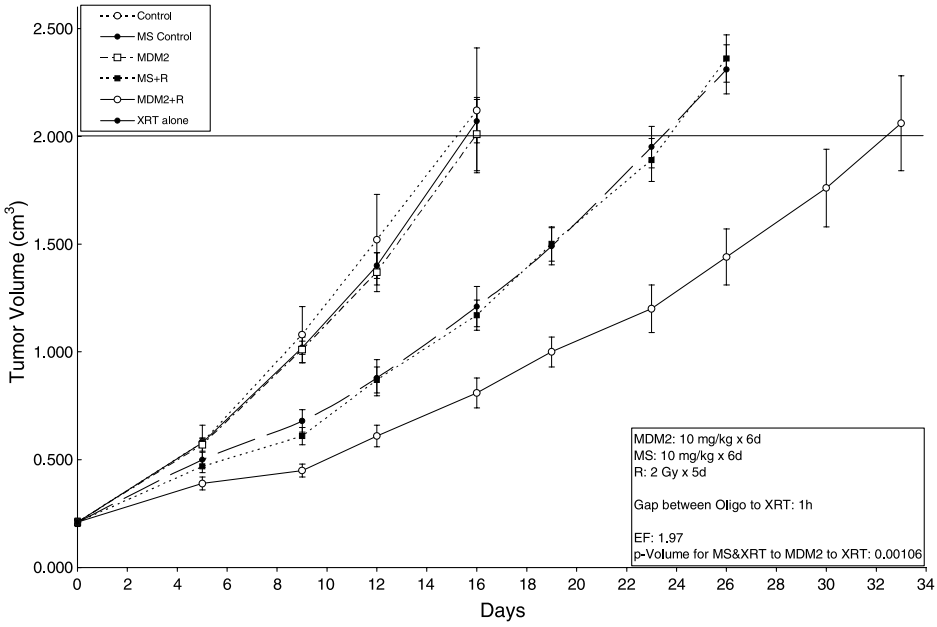

Figure 3. ASODNs against MDM2 radiosensitize H460 xenografts. H460 tumors were implanted in the flank of nude mice (five mice per treatment group) and treated with 10 mg/kg of anti-MDM2 or missense oligonucleotide via daily i.p. injections for 6 consecutive days. Irradiated groups received 10 Gy in five fractions (2 Gy daily fractions) from days 2 to 6. Data was calculated as the percentage of the original (day 1) tumor volume. *Points,* percentage change in tumor volume for each treatment group; *bars,* SD.

showed a moderate amount of vascularity as indicated by the representative image of a control tumor at the onset of treatment (Fig. 6). Color pixel density, which is an indicator of *in vivo* tumor vascular density, and power weighted pixel density, which is an indicator of blood flow through the tumor, were both calculated. Power weighted pixel density for control mice showed a 28% reduction in blood flow as calculated by the following formula: (pretreatment power weighted pixel density − posttreatment power weighted pixel density) / pretreatment power weighted pixel density. Missense oligonucleotide alone and anti-MDM2 oligonucleotide alone showed a 29% and a 47% reduction in blood flow, respectively. Missense oligonucleotide with radiation and anti-MDM2 oligonucleotide with radiation showed a 45% and a 64% reduction in blood flow, respectively ($P < 0.023$). Color pixel density values for control mice showed a 9% reduction in vascularity; missense oligonucleotide alone and anti-MDM2 oligonucleotide alone showed an 8% and 18% reduction in vascularity, respectively. Missense oligonucleotide with radiation and anti-MDM2 oligonucleotide with radiation showed a 14% and 34% reduction in vascularity, respectively ($P < 0.04$).

Discussion

This study suggests that inhibition of MDM2 via ASODN increases p21 and p53 levels, which results in increased cell death and radiosensitization of H460 lung cancer cells. It also suggests that an ASODN can be used as an antiangiogenic agent. The mechanisms by which MDM2 inhibition caused decreased tumor growth may be mediated by apoptosis and senescence.

H460 lung cancer cells treated with MDM2 ASODN had an increased level of p53 and p21. This may be important because decreased levels of p53 and p21 in malignancies have been shown to increase cancer cell resistance to the cytotoxic effects of chemotherapy or radiotherapy (5, 19–22). This is in agreement with previous studies that have shown an increase in p53 and p21 levels with the inhibition of MDM2 in several cancer cell lines (23). We have also shown that the novel MDM2 inhibitor, nutlin 3a, produces similar results with decreased MDM2 expression and increased p53 and p21 expressions.[3] Using p53-defective Val[138] lung cancer cells, we were also able to show that p53 expression was important in the response of cancer cells to both radiation and MDM2 inhibition.[3] MDM2 expression suppresses p53, attenuating p53 functions in cell cycle arrest, apoptosis, and response to DNA damage (24–27). Ionizing radiation activates p53, causing cell cycle arrest and apoptosis. On the other hand, ionizing radiation also activates MDM2 in a p53-dependent fashion, which attenuates p53-induced cell cycle arrest and apoptosis (6, 28, 29). MDM2 activation may play a critical role in preventing uncontrolled cell death caused by p53 in response to radiation (30). MDM2 antagonizes p53 by increasing its degradation (7, 31) and promotes its translocation from the nucleus to the cytoplasm (32). Furthermore, previous studies have suggested that restoring the balance between p53 and MDM2 either by inhibiting MDM2 activity or restoring p53 function by transfection with wild-type p53 can enhance radiosensitivity (33). Western blot analysis showed that anti-MDM2 oligonucleotide was sufficient to decrease MDM2 levels and to increase p53 levels in agreement with previous studies.

MDM2 inhibition seems to induce apoptosis and senescence. Clonogenic data indicated that H460 cells treated with anti-MDM2 had a decreased survival fraction; however, the

[3] B. Lu, unpublished data.

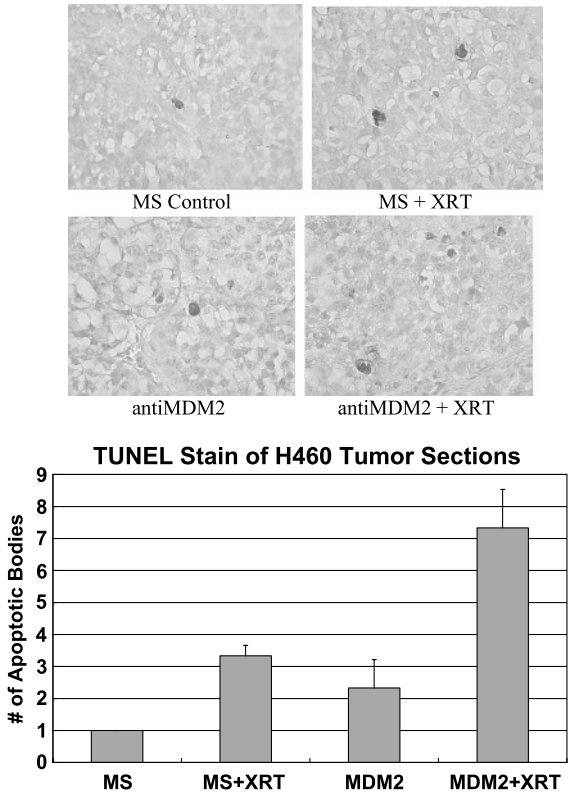

Figure 4. TUNEL staining of H460 tumors in nude mice. H460 cells were implanted into the flank of nude mice and grown for 8 d. Treatment with anti-MDM2 or missense oligonucleotide was given i.p. at a dose of 10 mg/kg for 6 d, 1 h before radiation. Radiation to a total dose of 10 Gy was given as 2 Gy daily fractions on treatment days 2 to 6. Animals were then sacrificed and tumors were TUNEL stained. Shown are representative photographs of TUNEL-stained tumors treated with anti-MDM2 oligonucleotide, missense oligonucleotide, anti-MDM2 oligonucleotide and radiation, and missense oligonucleotide and radiation. Apoptotic bodies were then counted (×100) in three separate, randomly selected fields. *Columns,* mean; *bars,* SD.

specific mechanism cannot be defined by the clonogenic assay. A significant increase in apoptosis was observed in cells treated with anti-MDM2 oligonucleotide and radiation, compared with anti-MDM2 oligonucleotide or missense oligonucleotide with radiation ($P < 0.05$). This was confirmed in the *in vivo* models. H460 tumors grown in nude mice showed a significant increase in TUNEL staining in mice treated with anti-MDM2 oligonucleotide with radiation compared with anti-MDM2 alone ($P < 0.02$).

Previous studies have suggested that p53 expression may play an important role in cell senescence and life span (34, 35). Further studies showed that p21 is important in the maintenance and induction of senescence (36, 37). Our study indicated that MDM2 inhibition, in conjunction with radiation, was sufficient for induction of senescence, possibly due to increased p53 and p21 levels induced by MDM2 inhibition. This is in agreement with studies that have shown that p21 and p53 are sufficient for cell senescence.

MDM2 is an important target for improving radiotherapy of lung cancer. MDM2 inhibition resulted in increased cell death as measured by apoptosis and cell senescence; it decreases survival of lung cancer cells in culture following irradiation. Administration of MDM2 ASODN during radiotherapy of H460 xenografts further delayed tumor growth, which may be explained by direct enhancement of cytotoxic effect on tumor cells, as shown by TUNEL staining, or by augmented antivascular effects, as shown by Doppler studies.

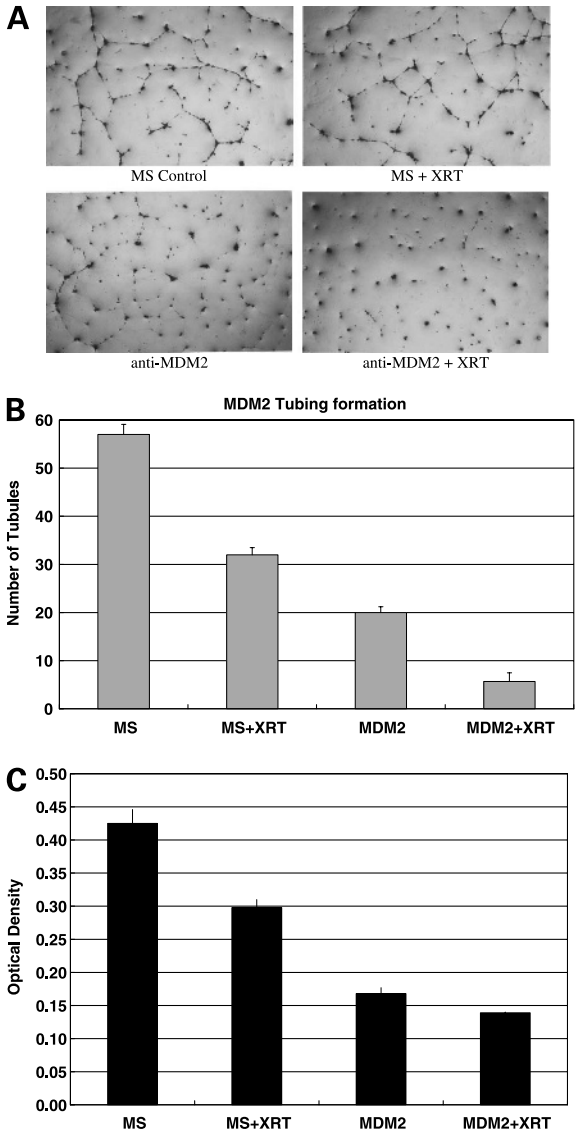

Figure 5. Endothelial cell tubule formation. HUVECs transfected with anti-MDM2 or missense oligonucleotide were irradiated with 0 or 3 Gy as indicated. Cells were trypsinized and 4.8×10^4 cells were resuspended in standard medium. Cells were plated on 24-well plates coated with Matrigel. After 6 h, cells were fixed and stained with H&E. The slides were examined by microscopy (×100). Stained tubules were then counted in three separate, randomly selected fields; representative fields are shown (**A**). *Columns,* mean; *bars,* SD (**B**). HUVEC viability was determined with treatment with MTT, which is converted to purple formazan dye by viable cells overnight. Cell viability is assessed by quantifying the dye at an absorbance of 570 nm (**C**). All samples were done in triplicate.

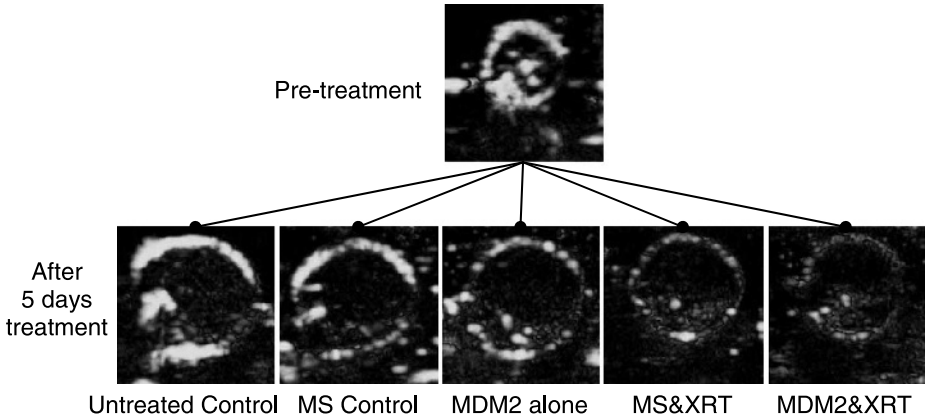

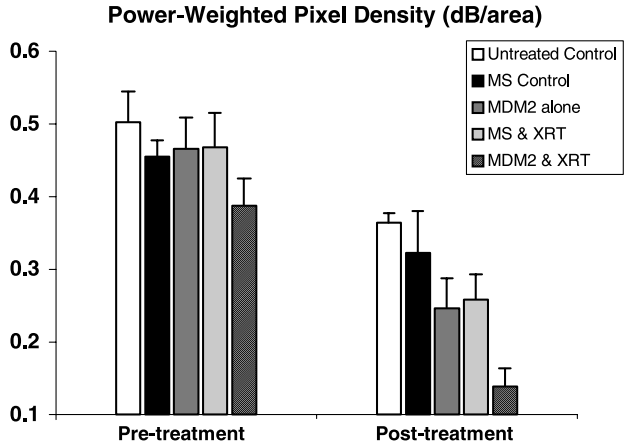

Figure 6. Quantification of blood flow via color power Doppler images. Shown are representative color power Doppler images of tumors before treatment and 5 d after treatment with missense oligonucleotide, anti-MDM2 oligonucleotide, missense oligonucleotide with radiation, anti-MDM2 oligonucleotide with radiation, and untreated control. Each treatment group was comprised of five mice. Shown are changes in flow, expressed as a percentage of day 1 flow, from days 1 to 5 for the above four treatment groups. *Columns,* mean; *bars,* SD.

p53 has been shown to induce the expression of angiogenesis inhibitors, such as thrombospondin-1, and decrease the expression of the vascular endothelial growth factor (38–42). In the present study, HUVEC treated with MDM2 ASODNs showed a decrease in MDM2 expression. p53 was increased in anti-MDM2 oligonucleotide–treated HUVEC, which is expected with the decrease in MDM2. This increase in p53 may be causing the decreased HUVEC viability, but other factors may be involved. Western blots showed little difference in MDM2 expression in HUVEC treated with anti-MDM2 oligonucleotide compared with those treated with anti-MDM2 oligonucleotide and radiation. *In vitro* Matrigel analysis showed impaired tubule formation, which may be the result of decreased HUVEC viability as shown by the MTT assay. It is likely that radiation decreases HUVEC viability in non-p53–dependent ways. Radiation can cause p53 activation by causing DNA double-stranded breaks; however, if p53 has already been activated to a large degree by anti-MDM2 oligonucleotide, the increase in p53 induced by radiation may not be readily apparent. However, DNA double-strand breaks can also activate a variety of other DNA repair mechanisms that can halt the cell cycle and affect HUVEC viability, such as ATR, ATM, and DNA-PK. The activation of these repair mechanisms accounts for the difference in viability seen between HUVEC treated with anti-MDM2 alone compared with those treated with radiation and anti-MDM2 oligonucleotide. *In vivo* (Doppler) data suggest that anti-MDM2 oligonucleotide enhanced antivascular effects of radiation. Therefore, clinical studies using similar strategies that use agents targeting MDM2 and p53 interactions (30, 31) should be considered for patients with locally advanced non–small cell lung cancer who are currently treated with standard thoracic radiotherapy in combination with chemotherapy.

However, limitations of such clinical studies must be considered. For example, it has been shown that MDM2 and p53 mutations generally do not occur in the same tumor, and that most tumors with amplification of MDM2 have wild-type p53 (23). However, MDM2-targeted therapy may not be effective in tumors with p53 mutation or inactivation. Furthermore, caution must be taken due to the radiosensitization of normal lung tissues during such combined therapy. More rigorous preclinical studies on normal lung tissue injury from such combined therapy should be conducted. Clinical studies using combined radiotherapy and MDM2 inhibitors may require more precise tumor targeting and normal tissue sparing.

References

1. Wang H, Nan L, Yu D, Agrawal S, Zhang R. Antisense anti-MDM2 oligonucleotides as a novel therapeutic approach to human breast cancer: *in vitro* and *in vivo* activities and mechanisms. Clin Cancer Res 2001;11:3613 – 24.

2. Freedman DA, Levine AJ. Regulation of the p53 protein by the MDM2 oncoprotein—thirty-eighth G.H.A. Clowes Memorial Award lecture. Cancer Res 1999;1:1 – 7.

3. Woods DB, Vousden KH. Regulation of p53 function. Exp Cell Res 2001;1:56 – 66.

4. Wang H, Oliver P, Zhang Z, Agrawal S, Zhang R. Chemosensitization and radiosensitization of human cancer by antisense anti-MDM2 oligonucleotides: *in vitro* and *in vivo* activities and mechanisms. Ann N Y Acad Sci 2003;1002:217 – 35.

5. Zhang Z, Wang H, Li M, Agrawal S, Chen X, Zhang R. MDM2 is a negative regulator of p21WAF1/CIP1, independent of p53. J Biol Chem 2004;16:16000 – 6.

6. Chen J, Wu X, Lin J, Levine AJ. mdm-2 inhibits the G1 arrest and apoptosis functions of the p53 tumor suppressor protein. Mol Cell Biol 1996;5:2445 – 52.

7. Haupt Y, Maya R, Kazaz A, Oren M. Mdm2 promotes the rapid degradation of p53. Nature 1997;6630:296 – 9.

8. Mu Z, Hachem P, Agrawal S, Pollack A. Antisense MDM2 sensitizes prostate cancer cells to androgen deprivation, radiation, and the combination. Int J Radiat Oncol Biol Phys 2004;2:336 – 43.

9. Dilla T, Romero J, Sanstisteban P, Velasco JA. The mdm2 proto-oncogene sensitizes human medullary thyroid carcinoma cells to ionizing radiation. Oncogene 2002;15:2376 – 86.

10. Zhang Z, Li M, Wang H, Agrawal S, Zhang R. Antisense therapy targeting MDM2 oncogene in prostate cancer: Effects on proliferation, apoptosis, multiple gene expression, and chemotherapy. Proc Natl Acad Sci U S A 2003;20:11636 – 41.

11. Dotto GP. p21(WAF1/Cip1): more than a break to the cell cycle? Biochim Biophys Acta 2000;1:M43 – 56.

12. Helene C, Toulme JJ. Specific regulation of gene expression by antisense, sense and antigene nucleic acids. Biochim Biophys Acta 1990; 2:99 – 125.

13. Peyman A, Helsberg M, Kretzschmar G, Mag M, Grabley S, Uhlmann E. Inhibition of viral growth by antisense oligonucleotides directed against the IE110 and the UL30 mRNA of herpes simplex virus type-1. Biol Chem Hoppe Seyler 1995;3:195 – 8.

14. Smith L, Andersen KB, Hovgaard L, Jaroszewski JW. Rational selection of antisense oligonucleotide sequences. Eur J Pharm Sci 2000;3:191 – 8.

15. Crooke ST. Progress in antisense therapeutics. Hematol Pathol 1995;2:59 – 72.

16. Chen L, Agrawal S, Zhou W, Zhang R, Chen J. Synergistic activation of p53 by inhibition of MDM2 expression and DNA damage. Proc Natl Acad Sci U S A 1998;1:195 – 200.

17. Edwards E, Geng L, Tan J, Onishko H, Donnelly E, Hallahan DE. Phosphatidylinositol 3-kinase/Akt signaling in the response of vascular endothelium to ionizing radiation. Cancer Res 2002;16:4671 – 7.

18. Geng L, Donnelly E, McMahon G, et al. Inhibition of vascular endothelial growth factor receptor signaling leads to reversal of tumor resistance to radiotherapy. Cancer Res 2001;6:2413 – 9.

19. Bao R, Connolly DC, Murphy M, et al. Activation of cancer-specific gene expression by the survivin promoter. J Natl Cancer Inst 2002;7: 522 – 8.

20. Rodel C, Haas J, Groth A, Grabenbauer GG, Sauer R, Rodel F. Spontaneous and radiation-induced apoptosis in colorectal carcinoma cells with different intrinsic radiosensitivities: survivin as a radioresistance factor. Int J Radiat Oncol Biol Phys 2003;5:1341 – 7.

21. Clarke AR, Purdie CA, Harrison DJ, et al. Thymocyte apoptosis induced by p53 dependent and independent pathways. Nature 1993; 6423:849 – 52.

22. Kastan MB, Onyekwere O, Sidransky D, Vogelstein B, Craig RW. Participation of p53 protein in the cellular response to DNA damage. Cancer Res 1991;23 Pt 1:6304 – 11.

23. Zhang Z, Wang H, Prasad G, et al. Radiosensitization by antisense anti-MDM2 mixed-backbone oligonucleotide in *in vitro* and *in vivo* human cancer models. Clin Cancer Res 2004;4:1263 – 73.

24. Vogelstein B, Kinzler KW. p53 function and dysfunction. Cell 1992; 4:523 – 6.

25. Livingstone LR, White A, Sprouse J, Livanos E, Jacks T, Tlsty TD. Altered cell cycle arrest and gene amplification potential accompany loss of wild-type p53. Cell 1992;6:923 – 35.

26. Kastan MB, Zhan Q, el-Deiry WS, et al. A mammalian cell cycle checkpoint pathway utilizing p53 and GADD45 is defective in ataxia-telangiectasia. Cell 1992;4:587 – 97.

27. Zakut-Houri R, Bienz-Tadmor B, Givol D, Oren M. Human p53 cellular tumor antigen: cDNA sequence and expression in COS cells. EMBO J 1985;5:1251 – 5.

28. Perry ME, Piette J, Zawadzki JA, Harvey D, Levine AJ. The *mdm-2* gene is induced in response to UV light in a p53-dependent manner. Proc Natl Acad Sci U S A 1993;24:11623 – 7.

29. Chen CY, Oliner JD, Zhan Q, Fornace AJ Jr, Vogelstein B, Kastan MB. Interactions between p53 and MDM2 in a mammalian cell cycle checkpoint pathway. Proc Natl Acad Sci U S A 1994;7:2684 – 8.

30. Perry ME. Mdm2 in the response to radiation. Mol Cancer Res 2004; 1:9 – 19.

31. Kubbutat MH, Jones SN, Vousden KH. Regulation of p53 stability by Mdm2. Nature 1997;6630:299 – 303.

32. Freedman DA, Levine AJ. Nuclear export is required for degradation of endogenous p53 by MDM2 and human papillomavirus E6. Mol Cell Biol 1998;12:7288 – 93.

33. Grunbaum U, Meye A, Bache M, et al. Transfection with mdm2-antisense or wtp53 results in radiosensitization and an increased apoptosis of a soft tissue sarcoma cell line. Anticancer Res 2001;3B: 2065 – 71.

34. Maier B, Gluba W, Bernier B, et al. Modulation of mammalian life span by the short isoform of p53. Genes Dev 2004;3:306 – 19.

35. Ghosh A, Stewart D, Matlashewski G. Regulation of human p53 activity and cell localization by alternative splicing. Mol Cell Biol 2004;18:7987 – 97.

36. Brown JP, Wei W, Sedivy JM. Bypass of senescence after disruption of *p21CIP1/WAF1* gene in normal diploid human fibroblasts. Science 1997;5327:831 – 4.

37. Gire V, Wynford-Thomas D. Reinitiation of DNA synthesis and cell division in senescent human fibroblasts by microinjection of anti-p53 antibodies. Mol Cell Biol 1998;3:1611 – 21.

38. Dameron KM, Volpert OV, Tainsky MA, Bouck N. Control of angiogenesis in fibroblasts by p53 regulation of thrombospondin-1. Science 1994;5178:1582 – 4.

39. Van Meir EG, Polverini PJ, Chazin VR, Su Huang HJ, de Tribolet N, Cavenee WK. Release of an inhibitor of angiogenesis upon induction of wild type p53 expression in glioblastoma cells. Nat Genet 1994;2:171 – 6.

40. Mukhopadhyay D, Tsiokas L, Sukhatme VP. Wild-type p53 and v-Src exert opposing influences on human vascular endothelial growth factor gene expression. Cancer Res 1995;24:6161 – 5.

41. Bouvet M, Ellis LM, Nishizaki M, et al. Adenovirus-mediated wild-type p53 gene transfer down-regulates vascular endothelial growth factor expression and inhibits angiogenesis in human colon cancer. Cancer Res 1998;11:2288 – 92.

42. Fontanini G, Boldrini L, Vignati S, et al. Bcl2 and p53 regulate vascular endothelial growth factor (VEGF)-mediated angiogenesis in non-small cell lung carcinoma. Eur J Cancer 1998;5:718 – 23.

Molecular Cancer Therapeutics

Murine double minute 2 as a therapeutic target for radiation sensitization of lung cancer

Carolyn Cao, Eric T. Shinohara, Kenneth J. Niermann, et al.

Mol Cancer Ther 2005;4:1137-1145.